ACS OMEGA

Open Access

http://pubs.acs.org/journal/acsodf

Article

Unveiling the Microscopic Origin of Ion Transference Numbers in Molten Salt Systems: A Kinetic Theory Approach to an Accurate "Golden Rule"

Aïmen E. Gheribi*

Cite This: *ACS Omega* 2025, 10, 10272−10282

Read Online

ACCESS | Metrics & More | Article Recommendations | Supporting Information

ABSTRACT: In recent years, there has been a renewed interest in accurately quantifying the ion's transference number within molten salts. Surprisingly, despite efforts to address the severe lack of experimental data, there is still no reliable theoretical framework that establishes a clear link between the transference number and simulated phase trajectories through atomistic simulations or a dependable theoretical relationship for precise estimation. In general, overcoming limitations in both experimental and fundamental aspects, transference numbers are typically estimated by either considering the Nernst−Einstein (NE) approximation or employing the so-called "golden rules". However, it is worth noting that neither the Nernst−Einstein approximation nor the "golden rules" provide a truly accurate prediction. This work concentrates on establishing a robust theoretical framework to accurately define transference number boundaries and averages within molten salt systems. This is achieved by integrating principles from kinetic theory with an in-depth exploration of the electronic structure and local ordering of molten salts. Unlike prevailing theoretical approaches that are heavily reliant on Einstein's concept of ion mobility, which correlate with self-diffusion, the proposed theoretical framework is fundamentally grounded in the inherent mobility of ions. In summary, the introduction of this original "golden rule" showcases robust predictive capabilities, effectively addressing the scarcity of diverse observations gleaned from various experimental sources in the literature. Finally, the proposed formalism is extended to complex molten salts through a microscopic consideration of the impact of the cation associated with the anion upon its diffusional cross-section. Based on this, the cationic transference number of all divalent metal halide molten salts is predicted to be very close to that reported in the literature.

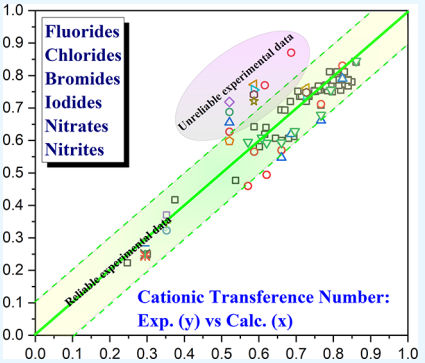

INTRODUCTION

External transport numbers, referred to as transference numbers (t_i), provide a practical representation of how individual ions uniquely impact the overall ionic conductivity.[1,2] Their significance spans fundamental, practical, and industrial applications, particularly in the realm of electrochemistry and processes involving wear and corrosion. Even today, quantifying the transference number for simple molten salt mixtures remains a challenging task from both experimental and simulation perspectives. Experimental data on molten salt mixtures are scarce, mostly outdated, dating back to the 1980s, and widely scattered. While claiming a maximum relative error of approximately ±20%, these data sets exhibit significant dispersion among them.[3−5]

On the simulation front, accurately predicting the total conductivity of molten salt mixtures typically relies on equilibrium molecular dynamics (EMD) simulations. These simulations necessitate a reliable force field to describe ion interactions and generate phase trajectories over an extended period, usually spanning a few nanoseconds. While EMD simulations are commonly employed to determine total conductivity through phase trajectories derived via the Green−Kubo (GK) method, a comprehensive extension of this approach to partial conductivities and transference numbers is still lacking. The absence of a reliable theoretical framework connecting partial conductivities to simulated phase trajectories highlights a critical gap in the field.

Currently, the only partial transport parameter that can be predicted via the EMD and GK methods is the self-diffusion coefficient, from which partial ion conductivities can be estimated using the Nernst−Einstein approximation, which assumes uncorrelated ions. However, this approximation has proven inaccurate, showing significant discrepancies with experimental data sets for both simple (fully dissociated) and complexing molten salts. These discrepancies underscore the importance of ion−ion correlations in the charge transport mechanism.

Received: October 25, 2024
Revised: January 31, 2025
Accepted: February 5, 2025
Published: March 3, 2025

Traditionally, transference numbers have been estimated using semiempirical methods, such as the "golden rules," which relate these values to fundamental ion properties like mass and radius. However, these methods often yield inconsistent results and lack the precision required for both dissociated and complexed molten salt systems.

This study aims to bridge this gap by proposing a robust "golden rule" grounded in kinetic theory. By establishing a connection between the ion's collision cross-section and transference numbers, considering the local and electronic structure of ion pairs within the system, this work seeks to provide a reliable theoretical framework that surpasses the limitations of current empirical approaches. The proposed framework results in the formulation of an original "Golden Rule" that offers enhanced predictive accuracy for predicting the transference numbers of ions in monovalent and divalent metal halide molten salt compounds and mixtures.

PROBLEM OF QUANTIFYING ION TRANSFERENCE NUMBERS IN MOLTEN SALTS AND PROPOSITION OF A ROBUST "GOLDEN RULE"

Transference numbers serve as a measure of an ion's contribution to the overall conductivity of a system. These are derived from the ratio between an ion's partial conductivity (σ_i) and the total conductivity (σ) in a solution. An alternative, more tangible interpretation of transference numbers stems from an ion's mobility (μ_i), establishing a direct connection between the movement of charges and their velocity under an applied electric field:[6]

$$t_i = \frac{\sigma_i}{\sigma} = \frac{\sigma_i}{\sum_i \sigma_i} = \frac{z_i c_i \mu_i}{\sum_i z_i c_i \mu_i} \tag{1}$$

where c_i and z_i represent the concentration and the charge of the species i, respectively. The calculation of total conductivity from simulated phase trajectories is commonly carried out within the Green−Kubo (GK) framework.[7] This method relies on Onsager's phenomenological coefficients[8] (L^{ij}) to establish the relationship with the total ionic conductivity, defined as follows:[9]

$$\sigma = F^2 \left(\sum_{i=1}^{N} z_i^2 L^{ii} + 2 \sum_{\substack{ij \\ j \neq i}} z_i z_j L^{ij} \right) \tag{2}$$

Here, F represents the Faraday constant, and N denotes the number of ions involved in the molten salt system. The determination of Onsager's phenomenological coefficients for an i−j pair, involving ions i and j, relies on the fluxes of both ions, $\mathbf{J}_i$ and $\mathbf{J}_j$. These ion fluxes are typically derived from the difference between each ion's velocity and the system's mass-averaged velocity. However, in practical applications, it is often more convenient to define these fluxes, and consequently, the Onsager coefficients, utilizing the mean-squared displacement of particle positions.[9]

$$\begin{aligned} L^{ij} &= \frac{V}{3k_B T} \int_0^\infty \langle \mathbf{J}_i(t) \cdot \mathbf{J}_j(0) \rangle \, dt \\ &= \frac{1}{6k_B TV} \lim_{t \to \infty} \frac{d}{dt} \Big\langle \sum_\alpha [\mathbf{r}_i^\alpha(t) - \mathbf{r}_i^\alpha(0)] \cdot \\ &\quad \sum_\beta [\mathbf{r}_j^\beta(t) - \mathbf{r}_j^\beta(0)] \Big\rangle \end{aligned} \tag{3}$$

Here, V stands for the equilibrium volume, and r_i^α denotes the position relative to the system's center of mass for particle α of type i. It is important to note that the definition above is symmetric, showing $L^{ij} = L^{ji}$. This symmetry constitutes a fundamental aspect of the Onsager reciprocal relations. Unfortunately, contrary to the total ionic conductivity, no clear GK base has been proposed yet for the derivation of the partial conductivity (σ_i) and therefore for the transference number. Put simply, the GK approach does not enable the division of L^{ij} into distinct contributions from ion i and ion j. In the case of simple molten salts, where ions exist in a fully dissociated state without the formation of coordination complexes, a natural assumption would be the equitable division of coefficient L^{ij} between the respective ions i and j. According to the generalized Langevin equation,[10,11] it is been established that the equal split assumption within L^{ij} perfectly aligns with Sundheim's "golden rule".[12] This holds true regardless of the interaction's magnitude, encompassing dispersion and polarization effects between ions i and j. Sundheim's "golden rule" emerges from the integration of the generalized Drude theory with the principles of momentum conservation, the continuity equation for each species, and the electroneutrality constraint.[12] It is represented as $\sum c_i \, m_{c_i} \sigma_{c_i} = \sum_{a_j} m_{a_j} \sigma_{a_j}$, wherein c_i and a_j denote the respective cation c_i and anion a_j. When considering compounds composed of a monovalent cation and a monovalent anion (e.g., alkali halides like NaCl, LiF, etc.), employing the equal split assumption in L^{ij} allows for the expression of both the anionic and cationic transference numbers as

$$\textbf{C.1:} \begin{cases} -2\, L^{+-} \nearrow & -1\, L^{+-} \to \sigma_+ \\ & -1\, L^{+-} \to \sigma_- \end{cases} \Leftrightarrow \begin{cases} \sigma_+ = F^2 (L^{++} - L^{+-}) \\ \sigma_- = F^2 (L^{--} - L^{+-}) \end{cases}$$

$$\Leftrightarrow \begin{cases} t_+ = m_- / (m_- + m_+) = t_+^{Sund.} \\ t_- = m_+ / (m_- + m_+) = t_-^{Sund.} \end{cases}$$

Figure 1 presents the cation transference number in alkali halides, derived from EMD calculations of the Onsager phenomenological coefficient when assuming an equal split of the coefficient L^{+-} between the cation and anion, in comparison with predictions made using the Sundheim's "golden rule".[12] The EMD simulations are performed in the canonical ensemble starting from an initial thermally equilibrated configuration. Detailed simulation parameters and specifications, including information on the force field governing interactions, are provided in the Supporting Information. To analyze the impact of the temperature on **C.1**, three distinct temperatures have been considered: T_m + 25 K, 1300 K, and T_m + 200 K (where T_m is the melting temperature). Remarkably, the assumption of an equal split of the L^{+-} Onsager coefficient between the cation and the anion exactly aligns with Sundheim's golden rule[12] for alkali halides, irrespective of temperature or system variations

https://doi.org/10.1021/acsomega.4c09587
ACS Omega 2025, 10, 10272−10282

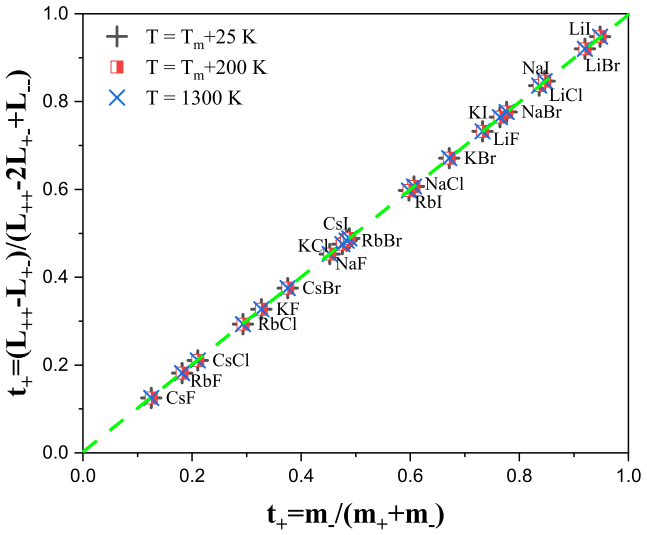

Figure 1. Comparison of EMD-calculated cation transference numbers at three distinct temperatures (T_m + 25 K, 1300 K, and T_m + 200 K) for alkali halides. Assessing the impact of the equal split assumption for the L^{ij} Onsager coefficient against Sundheim's "golden rule".

(regardless the nature and magnitude of the interactions). Sundheim's golden rule frequently fails to predict ionic transfer numbers, particularly when there's a considerable difference in mass between cations and anions, as seen in Figure 2. It remains noteworthy that today the relationship between transference number and EMD simulations still heavily relies on the assumption of equal splitting within the Onsager cross-term coefficient. This perpetuates a misconception that Sundheim's "golden rule"[12] is inherently tied to the GK (Green−Kubo) method used in analyzing phase trajectories.[7,9] However, it is crucial to clarify that, strictly speaking, the GK method does not allow for the prediction of partial ionic conductivity; rather, it exclusively focuses on estimating total conductivity.[7,9] Although there are modifications of Onsager's transport coefficients aimed at improving the prediction of transference numbers from EMD simulations, these methods generally have a limited range of applicability. They are confined to specific cases, such as complex molten salt mixtures with a singular free cation. In our work, we do not aim to propose an alternative expression of the partial conductivity based on the Onsager coefficients. Rather, our objective is to comprehend the microscopic origins behind the deviation from Sundheim's "golden rule" observed in the majority of experimental studies. The approach presented here is built upon the self-diffusion coefficient, D_i, representing a singular dynamic property associated with individual charges. Unlike the total conductivity, this specific property is accessible uniquely through the GK analysis of phase trajectories simulated by EMD. When the periodic boundary conditions (PBC) are applied, the calculation of D_i can be derived directly via Einstein's relation. This relation establishes a clear correlation between the root mean squared displacement of charges and the self-diffusion coefficient:[13,14]

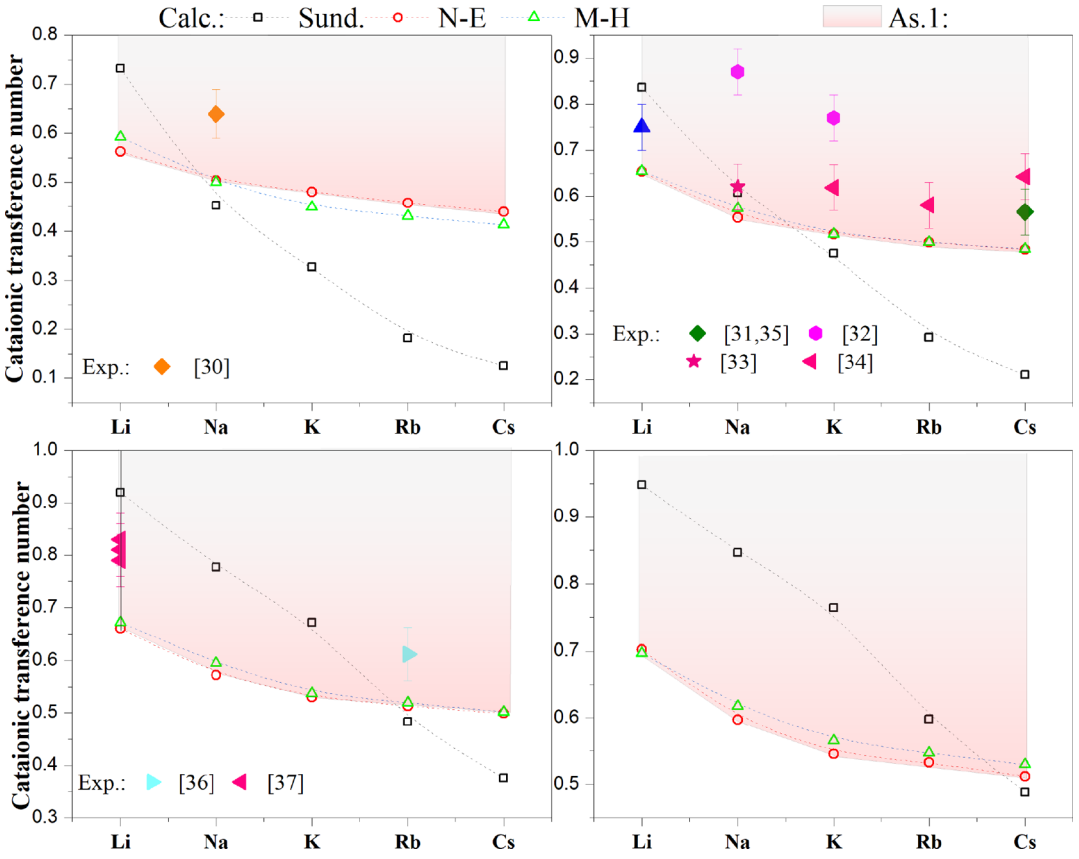

Figure 2. Comparison of calculated cationic transference numbers in simple alkali halides 25 K above their melting temperature using Sundheim's and Mulcahy-Heymann's "golden rules" against the Nernst−Einstein approximation and extensive experimental data. The shaded area denotes assumption **As.1** proposed in this study. Nernst−Einstein cationic transference numbers were computed using self-diffusion coefficients obtained from eqs 4 and 5, derived from phase trajectories via EMD simulations (refer to Supporting Information). Experimental data sources: refs 30−37.

https://doi.org/10.1021/acsomega.4c09587
ACS Omega 2025, 10, 10272−10282

$$D_i^{PBC} = \frac{1}{N_i}\frac{1}{6}\lim_{t\to\infty}\frac{\mathrm{d}}{\mathrm{d}t}\left\langle \sum_{\alpha}\left[\mathbf{r}_i^{\alpha}(t) - \mathbf{r}_i^{\alpha}(0)\right]^2\right\rangle \tag{4}$$

Subsequently, in order to mitigate the box length dependency caused by the periodic boundary conditions on the EMD simulated diffusion coefficient D_i^{PBC}, corrections by Dünweg and Kremer are employed:[15−18]

$$D_i^0 = D_i^{PBC} + \frac{k_B T\xi}{6\pi\eta L} \tag{5}$$

with ξ set at 2.837297 and η symbolizing the viscosity obtained from the phase trajectories akin to D_i^{PBC}, L represents the length of the (cubic) simulation box. Note that the Dünweg and Kremer correction stems from the kinetic theory framework and employs the Stokes law to delineate the frictional electrostatic forces exerted on ion i. The Nernst−Einstein approximation, assuming entirely uncorrelated ion motion aligned with the concept of a dilute ideal solution, associates the ion's mobility with the self-diffusion coefficient and, consequently, with the transference number:

$$\mu_i^{NE} = \frac{z_i F}{RT} D_i^0 \Rightarrow t_i^{NE} = \frac{z_i y_i D_i^0}{\sum_i z_i y_i D_i^0} \tag{6}$$

$y_i = n_i/\sum_i n_i$ being the molar fraction of the charge carrier i. It is important to note that t^{NE} is commonly referred to as t^{NMR} since it represents the transference number typically derived from nuclear magnetic resonance (NMR) experiments.[19−21] In standard solvents, transport numbers are typically defined with regard to the solvent itself, which is generally assumed to remain immobile on average in the presence of an electric field. However, in the absence of a solvent, it becomes more appropriate to attribute a similar significance to the anions, particularly considering that variations in composition predominantly involve changes in the cationic component. According to Gheribi et al.'s proposal, it is plausible to consider that, compared to uncorrelated ions, electrostatic interference amplifies the relative mobility of cations at the cost of the anions.[9,22] Put differently, one might infer that the Nernst−Einstein relation aligns with the minimum transference number for the cation and the maximum for the anion. This concept can be encapsulated through the following assumption (**As.1**) regarding the minimum cationic and maximum anionic transference numbers:

$$\textbf{As.1:}\begin{cases} min\ t_{c_i} = t_{c_i}^{NE} \\ max\ t_{a_j} = t_{a_j}^{NE} \end{cases}$$

Paradoxically, while efforts to expand beyond the Nernst−Einstein definition of transference numbers for molten salts persist, they remain anchored in kinetic theory and revolve around considering the self-diffusion coefficient. Within the realm of kinetic theory, the Einstein-Sutherland interpretation of the self-diffusion coefficient reveals its inverse proportionality to an effective electrostatic friction coefficient (ς_i), quantifying the resistance encountered by ion i during its motion through the medium: $D_i^0 = k_B\ T/\varsigma_i$.[23,24] Following the consideration of ions as spherical entities and the application of Stokes's empirical law[25] to define ς ($\varsigma_i = b\ \pi\ \eta\ R_i^H$, where R_i^H represents the hydrodynamic radius of ion i and b signifies a constant defining the boundary condition at the particle−solvent interface), Mulcahy and Heymann (MH) suggested that, within a single molten compound consisting of one anion and one cation, the ratio of ion velocities might be inversely proportional to their effective average radius ($\overline{r}_i$)![26] MH's assumption arises from balancing electrostatic friction with that resulting from the applied electric field, leading directly to the establishment of the widely acknowledged "golden rule" for the cationic transference number for a single molten compound:

$$t_+^{MH} = \frac{z_+\overline{r}_-}{z_+\overline{r}_- + z_-\overline{r}_+} \tag{7}$$

Beyond the force equilibrium, MH can be extended and generalized to higher-order systems using kinetic theory in tandem with the Nernst−Einstein approximation for uncorrelated systems. The amalgamation of the Stokes−Einstein approximation for self-diffusion coefficients and the Nernst−Einstein approximation for transference numbers results in

$$D_i^0 = \frac{k_B T}{b\pi\eta r_i^H} \Rightarrow t_i^{MH} = \frac{z_i y_i (r_i^H)^{-1}}{\sum_i z_i y_i (r_i^H)^{-1}} \simeq \frac{z_i y_i (\overline{r}_i)^{-1}}{\sum_i z_i y_i (\overline{r}_i)^{-1}} \tag{8}$$

Note that, unlike Sundheim's approach, the mass of the ionic species does not factor into the MH expression for transference numbers. The cancellation of the mass term naturally arises from the force balance within Newton's law of motion. Initially, in comparison with experimental transference numbers, MH's "golden rule" seems to be a robust method for predicting the transference numbers of dissociated molten salts (i.e., those salts are not forming complexes) (Figure 2). In fact, it can be demonstrated that MH aligns entirely with NE, provided that the effective ionic radii are considered based on estimations within the molten state rather than the solid state. Typically, when attempting to establish a connection between the properties of molten salt mixtures and the ionic radii of their constituent ions, researchers often refer to Shannon's assessment.[27] Shannon's method[27] serves as a fundamental benchmark for the ionic radii utilized in electrochemistry, thermochemistry, and broader material science investigations. These radii incorporate considerations such as oxidation states, coordination numbers, electronic spin states in transition metals, covalency, repulsive forces, and polyhedral distortion. However, it is important to note that Shannon's ionic radii primarily reflect characteristics in the solid state rather than the liquid state, disregarding the specifics of the liquid phase.[27] Unlike Shannon's method, the Parrinello-Tosi approach takes into consideration the local structure, encompassing mean interionic distances and short-range ordering by correlating X-ray diffraction patterns, temperature-dependent molar volume, and compressibility with effective ionic radii.[28] It is important to note that Parrinello-Tosi's effective ionic radius is temperature-dependent, reflecting the decrease in density and velocity of sound of molten salt compounds as temperature changes.[29] In contrast, Shannon's ionic radius is assumed to remain constant and independent of temperature.[27] Under the prism of Parrinello-Tosi's definition and assessment of ionic radius,[28] it becomes apparent that the Mulcahy-Heymann approximation (eq 8) closely mirrors the Nernst−Einstein equation (eq 6) for a wide array of anion−cation pairs within dissociated molten salt compounds, as illustrated in Figure 2.

The self-diffusion coefficients used to derive t_+^{NE} were computed by integrating eqs 4 and 5 from phase trajectories simulated via EMD within the NVT statistical ensemble. The cationic transference number was evaluated at a temperature 25

https://doi.org/10.1021/acsomega.4c09587
ACS Omega 2025, 10, 10272−10282

K above the melting temperature, aligned with experimental temperature conditions. Detailed simulation parameters, including equilibrium density, self-diffusion coefficient, viscosity, and Parrinello-Tosi's radius[28] (to calculate t_+^{MH}) at T_m+25 K, are provided in the Supporting Information. The nearly precise alignment between MH and NE approximations does not necessarily imply that the Einstein-Stokes approximation of self-diffusion is entirely in line with that derived from EMD and therefore closely matches the experimental data. Rather, it indicates that the ratio between anionic and cationic hydrodynamic radii corresponds to that of Parrinello-Tosi's effective radius. Despite being scattered and often reported with considerable uncertainty, all experimental cationic transference numbers documented in the literature consistently surpass those predicted by both the NE and MH approximations, even when accounting for their wide error margins (Figure 2). The significant deviation from both NE and MH highlights substantial cation−anion correlations stemming from electrostatic interference. The observation that $t^{MH} \simeq t^{NE}$ suggests that the MH approximation fails to capture the pronounced cation−anion correlation influencing charge transport, even within simple molten salts. NE's limitation arises from the nearly identical magnitude of frictional electrostatic forces acting on both anion and cation, as determined by the system's total viscosity; this disregards the contribution of individual charge species' partial viscosity in the Stokes expression of frictional forces. Although kinetic theory provides explicit expressions for partial viscosity, they have not been integrated to refine the MH's model, likely due to the lack of experimental validation concerning the partial viscosity of mixed charge species. Clearly, exhibiting a pronounced dependence on cationic mass, Sundheim's assumption results in unrealistic estimations of the cation transference number, consequently affecting the anionic estimation as well. It is noteworthy that for NaCl, Sundheim's "golden rule" accurately predicts the transference number. In some other compounds, Sundheim's rule coincides with the NE and MH approximations, albeit coincidentally (Figure 2). The limitations of the two common "golden rules" and NE approximation in predicting the transference number are summarized as follows:

$$\textbf{C.2:}\ \begin{cases} t_i^{MH} \equiv t_i^{NE} \\ t_{c_i}^{Exp.} \gg t_{c_i}^{MH(NE)} \left(\text{i.e } t_{a_j}^{Exp.} \ll t_{a_j}^{MH(NE)}\right) \\ \left(\partial t_+^{Sun.}/\partial m_{c_i}\right) \gg \left(\partial t_+^{Exp.}/\partial m_{c_i}\right) \sim \left(\partial t_+^{Exp.(NE)}/\partial m_{c_i}\right) \end{cases}$$

After a thorough discussion concerning the strengths and limitations of the predominant methods for predicting transference numbers within molten salts, our attention now turns to the theoretical formulation of an alternative and a more precise "golden rule". Let us delve into an ideal scenario involving binary molten compounds, where there is no electrostatic interference, consisting solely of a single anion and cation. Our main focus is to deeply consider how pair interactions influence the transference number. For now, we are setting aside the consideration of three-body interactions and higher-order effects. In the realm of kinetic theory, when particles interact and collide, both momentum and energy are conserved during these collisions. The collision mean free path represents the average distance a particle covers between collisions. Larger particles experience more frequent collisions, resulting in a shorter mean free path. In this context, a fundamental assumption emerges: the mobility of ion i is expected to have a linear dependence on its collision mean free path, $\lambda_i^{coll.}$, which in turn is inversely proportional to the ion's collision cross-section, $\Gamma_i^{coll.}$,[38] i.e., $\lambda_i^{coll.} = (c_i\Gamma_i^{coll.})^{-1}$. Note that $\Gamma_i^{coll.}$, akin to the charge mobility, is an intrinsic property that is not contingent on the charge carrier concentration, unlike the average collision mean free path, which does depend on it. Within the context of a classical liquid containing charged hard spheres, $\Gamma_i^{coll.} = 4\,\pi\,\overline{r}_i^2$. From this, the following assumption can be inferred:

$$\textbf{As.2:}\ \left\{\mu_i \propto \Gamma_i^{coll.} \Rightarrow \mu_i \propto \frac{1}{\overline{r}_i^2}\right.$$

In the ideal system, assuming ions as hard spheres with undistorted electronic clouds, and building upon the aforementioned assumption, it can be demonstrated from eq 1 that the transference number of ion i within the $i_{\nu_i}i_{\nu_j}$ molten salt compounds (where ν_i and ν_j denote the stoichiometric coefficients) is expressed as

$$t_i(\overline{r}_i, \overline{r}_j) = \frac{z_i\nu_i/\overline{r}_i^2}{z_i\nu_i/\overline{r}_i^2 + z_j\nu_j/\overline{r}_j^2} \tag{9}$$

Even in the most basic portrayal of ions as hard spheres interacting via Coulombic forces, the average ion size is not an inherent property, but rather influenced by its surroundings. In reality, a cation's polarizing power involves modifying an anion's electronic cloud. Typically, smaller and highly charged cations exhibit greater polarizing power. Conversely, polarizability denotes an anion's susceptibility to distortion by cations, with larger and less electronegative anions showing higher polarizability.[39] Understanding how an anion deforms under a cation's electrostatic influence also involves considering electronegativity. An ion's electronegativity, whether cation or anion, profoundly affects its interactions with neighboring ions; a higher electronegativity attracts electrons more strongly, influencing the ability to deform nearby ions. Regarding deformed ions as persistently behaving akin to hard spheres, the estimation of the effective radius for the deformed anion can be derived by considering the combined influence of electronegativity (χ) and polarizability (α) factors pertaining to both the anion and cation, as expressed in the following relationship:[40]

$$\overline{r}_{\text{an.}}^{*} = \overline{r}_{\text{an.}} \cdot \left[1 + \phi_{an-cat} \cdot \sqrt{\frac{\alpha_{\text{cat}}\chi_{\text{cat.}}}{\alpha_{\text{an}}\chi_{\text{an.}}}}\right] \tag{10}$$

The function $0 \le \phi_{an-cat} \le 1$ is linked to the ratio of electrons potentially engaged in the deformed electronic cloud. A value of $\phi_{an-cat} = 1$ signifies the maximum deformation of the anion, where all electrons from the anion contribute to the deformed electronic cloud. Conversely, $\phi_{an-cat} = 0$ represents an underformed anion scenario ($\overline{r}_{an.}^{*} \equiv \overline{r}_{an.}$). Although it is conceivable to correlate ϕ_{an-cat} with the ionicity level of the molten compound by considering the electronegativities of the anions and cations via Fajan's rule,[41] for simplicity, let us assume $\phi_{an-cat} = 1/(n^* - 1)$, where n^* represents the principal quantum number of the cation. Consequently, we presume a complete deformation of the electronic cloud for F^-; similarly, other anions (Cl^-, Br^-, and I^-) within a volume range comparable to that of F^- are assumed deformable. This assumption implies that the inner electrons have an insignificant role in the anion's deformation influenced by the polarizing power of the cation. The extreme values of ϕ_{an-cat} allow the determination of both the upper and lower limits for the transference numbers of the

https://doi.org/10.1021/acsomega.4c09587
ACS Omega 2025, 10, 10272−10282

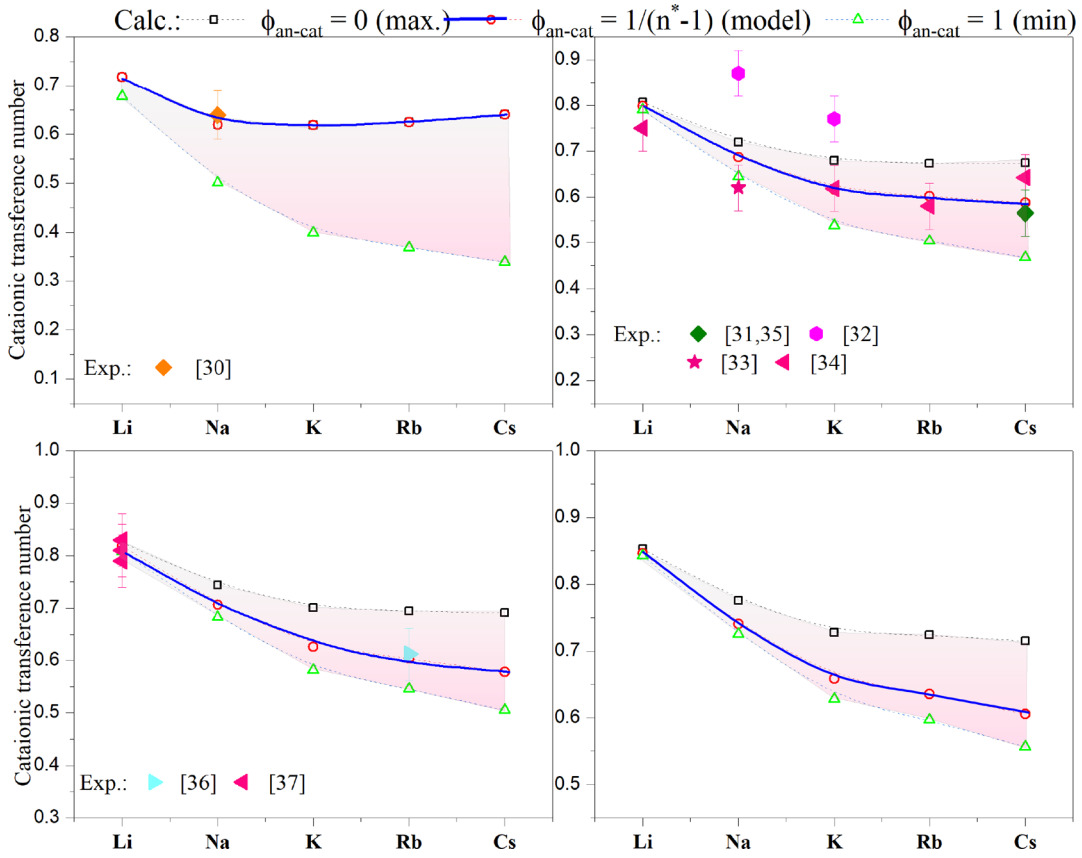

Figure 3. Comparison between the calculated upper and lower boundaries, along with the mean of the cationic transference numbers within alkali halides (fluorides, chlorides, bromides, and iodides), using the theoretical approach (eqs 9−11), against experimental data. The shadow area is defined as the domain encompassing the theoretical lower and upper limits, as described in eq 11. Experimental data sources: refs 30−37.

cation and anion within a specific molten salt compound. The assumed value of ϕ_{an-cat} $(1/(n^* - 1))$ defines the average transference number, $\langle t_i \rangle$, as

$$\begin{cases} t_{cat.}^{min} = t_{cat.}(\overline{r}_{cat.}, \overline{r}_{an.}^*) = 1 - t_{an.}^{max} \\ \quad \text{when } \phi_{an-cat} = 1 \\ \langle t_{cat.} \rangle = t_{cat.}(\overline{r}_{cat.}, \overline{r}_{an.}^*) = 1 - \langle t_{an.} \rangle \\ \quad \text{when } \phi_{an-cat} = 1/(n^* - 1) \\ t_{cat.}^{max} = t_{cat.}(\overline{r}_{cat.}, \overline{r}_{an.}^*) = 1 - t_{an.}^{min} \\ \quad \text{when } \phi_{an-cat} = 0 \end{cases} \tag{11}$$

RESULTS AND DISCUSSION

Figure 3 illustrates the calculated cationic transference numbers within molten halide compounds (fluorides, chlorides, bromides, and iodides) in comparison with all available experimental data sets in the literature, similar to Figure 2. Please note that the model parameters are provided in the Supporting Information. Except for the experimental data set by Duke and Cook,[32] all other experimental data sets available in the literature for molten alkali halides align with the theoretical boundaries outlined in eq 11. Additionally, a majority of the experimental data points fall remarkably close to the theoretical mean, often within the reported margins of experimental error. It is worth noting that the predicted trend in the means of the cationic transference numbers reveals a significant decrease from Li to Na or K, depending on the anion radius, followed by only a minor fluctuation in the cationic transference number. This behavior is observed experimentally in chlorides, where there's a wealth of reported experimental data available. The cationic transference number, and consequently the anionic transference number, remains relatively constant from NaF to CsF (approximately ∼0.64) in fluorides, characterized by the smallest anion. However, in iodides, featuring the largest halide anions, the cationic transference number experiences a significant decrease from LiI to KI, followed by a slight decline from KI to CsI. This trend can be explained by assuming a proportional relationship between ion mobility and diffusion cross-section, not through MH or NE, which predicts a monotonous variation in transference with cation size for a given halide anion. It is worth noting that all the predicted mean cationic transference numbers consistently exceed 0.6, which aligns with various experimental data sets but stands in contrast to the Nernst−Einstein approximation and other "golden rules".

Similar to chlorides, transference numbers have undergone extensive measurements within molten nitrate and nitrite compounds. However, these measurements date back several decades, with no recent experimental data published since. Unlike simple halide compounds where ions are completely dissociated, leading to the cation's polarizing power deforming and enlarging the effective size of the free anion and subsequently affecting the effective diffusional cross-section, NO_3^- and NO_2^- behave as complex anions. In these cases, the polarizing power of the free cation does not significantly alter their average size. By disregarding potential deformation in both

https://doi.org/10.1021/acsomega.4c09587
ACS Omega 2025, 10, 10272−10282

NO_3^- and NO_2^-, the transference numbers of nitrates and nitrites were computed using eq 9 and thermochemical radii of complex ions reported by Jenkins and Thakur.[48] They were plotted against available experimental data in Figure 4. Similar to

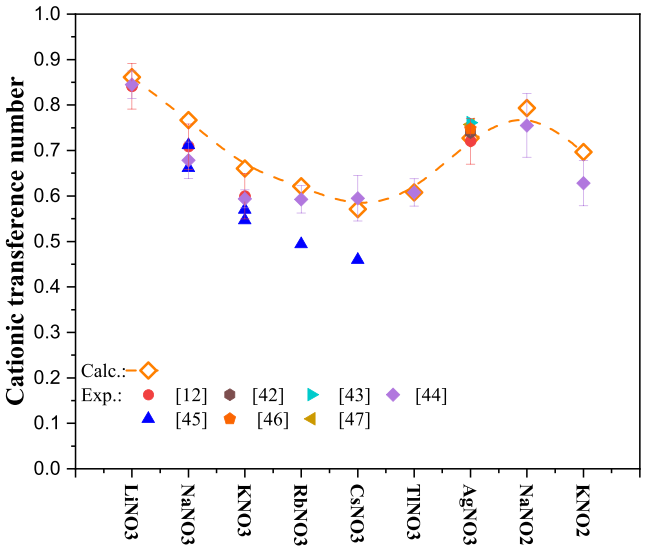

Figure 4. Comparison of calculated cationic transference numbers for alkali nitrates and nitrites, including $AgNO_3$ and $TlNO_3$, against available experimental data sets from literature. Experimental data sources: refs 12 and 42−47.

simple alkali halides, the predicted transference numbers closely align with most experimental findings, exhibiting notable disparity with only one data set reported by Honig in 1964[45] for $RbNO_3$ and $CsNO_3$. However, they remain close to other experimental data sets, falling within the margin of error.

The current theoretical framework remains valid for simple, dissociated, multicomponent molten salt mixtures excluding complex coordination and short-range ordering. Consider a multicomponent system sharing a common anion, such as $Ca^{(1)}An$-$Ca^{(2)}An$-···-$Ca^{(N)}An$ (e.g., LiCl-NaCl-KCl-... where $Ca^{(1)}$ = Li, $Ca^{(2)}$ = Na, $Ca^{(3)}$ = K, ... and Cl = An), showcasing a nonreciprocal arrangement. When neglecting electrostatic interference between cations, it is evident from eq 1 that both cationic and anionic transference numbers vary linearly with the volume fraction of the compound associated with the *i*th cation (e.g., NaCl):

$$\begin{cases} t_{Ca^{(i)}} = \phi_{Ca^{(i)}An} \cdot t_{Ca^{(i)}}^{Ca^{(i)}An} \\ t_{An} = \sum_{i=1}^{N} \phi_{Ca^{(i)}An} \cdot t_{An}^{Ca^{(i)}An} \end{cases} \quad (12)$$

where $\phi_{Ca^{(i)}An}$ stands for the volume fraction of the molten compound $Ca^{(i)}An$ in the multicomponent mixture, whereas $t_{Ca^{(i)}}^{Ca^{(i)}An}$ and $t_{An}^{Ca^{(i)}An}$ denote the specific cationic and anionic transference numbers within $Ca^{(i)}An$. It is essential to emphasize that the observed linear relationship between the transference number and the compound volume fraction arises from our assumption of consistent charge carrier mobility, a relationship directly associated with $1/r_i^2$ in our present model. Furthermore, it is noteworthy that across different compounds, both the cationic and anionic transference numbers can significantly vary, defined by the ratio of diffusion cross sections of the ions constituting the molten compound.

Figure 5 presents a comprehensive comparison between the calculated and experimental partial cationic transference numbers in the cases of NaCl-KCl, LiCl-KCl, NaCl-CsCl, and CsCl-LiCl and total cationic transference numbers for KBr-LiBr and RbBr-$BaBr_2$ systems, along with partial anionic transference numbers in the instances of NaF-NaCl and NaF-NaBr binary systems. Transference numbers were derived employing two distinct methodologies: (i) direct computation based on boundaries and means (refer to eq 11) incorporating cationic and anionic radii as defined by Parrinello-Tosi,[28] and (ii) application of eq 12, maintaining a constant transference number for the mixture's endmember as reported by experiments. This deliberate emphasis on composition dependence aims to facilitate a nuanced discussion on the validity of a linear relationship with the volume fraction of transference numbers in dissociated molten salt mixtures. In general, the establishment of linearity for both cationic and anionic transference numbers with respect to the volume fraction of the molten compound in the mixture is evident. However, it is noteworthy that a notable deviation is observed, particularly in the case of the transference number of Li^+ on the CsCl-rich side of the CsCl-LiCl system. Similarly, the transference number of Rb^+ in the $BaBr_2$-rich side of the RbBr-$BaBr_2$ system appears, at first glance, to be somewhat overestimated. In the majority of the systems, the raw predictions derived from eq 11, accounting for the deformation of the electronic cloud, closely align with experimental data. Any observed discrepancies are minimal and fall well within the margins of typical experimental error. The assumption that ion mobility is inversely proportional to its diffusion cross-section holds within the binary system. The chemical effect manifests solely in the variation of polarizing power perceived by the anion and the volumetric fraction of the compounds, equivalent to the volumetric concentration of the cation. The temperature dependence of the transference number is intricately connected to both the temperature-dependent ionic radius,[28] and the thermal expansion of the compounds comprising the mixture. These combined factors delineate the variation in the volumetric concentration of ions and the effective radius of anions with the temperature. In the LiCl-CsCl system, as reported by Smirnov et al.,[50] beyond X_{CsCl} = 0.6, the transference number of Li^+ diverges significantly from the expected curve based on eq 12. Closer to the CsCl-rich side, the transference number (t_{Li^+}) approaches near-null values, resulting in a minimal contribution of Li^+ to the overall conductivity of the system. This unexpected behavior, at first glance, can be attributed to the evolution of Li^+ within a dense coordination complex or a polymer chain associated with the anion. The presence of coordination complexes within the LiCl-CsCl molten mixture lacks experimental validation, as they have not been directly or indirectly observed. Besides experimental techniques, such as NMR spectroscopy, coordination complexes have not been directly identified by the current EMD simulations. They have also not been indirectly observed through viscosity or electrical conductivity measurements. If coordination complex formation had occurred, for instance, viscosity would have demonstrated a noticeable increase, while total conductivity would have shown a characteristic break. However, from an experimental point of view, these properties show a monotonic dependence on composition. That said, significant fluctuations in interionic distances, along with the overlapping of ion−ion and ion-dipole interactions, have been

https://doi.org/10.1021/acsomega.4c09587
ACS Omega 2025, 10, 10272−10282

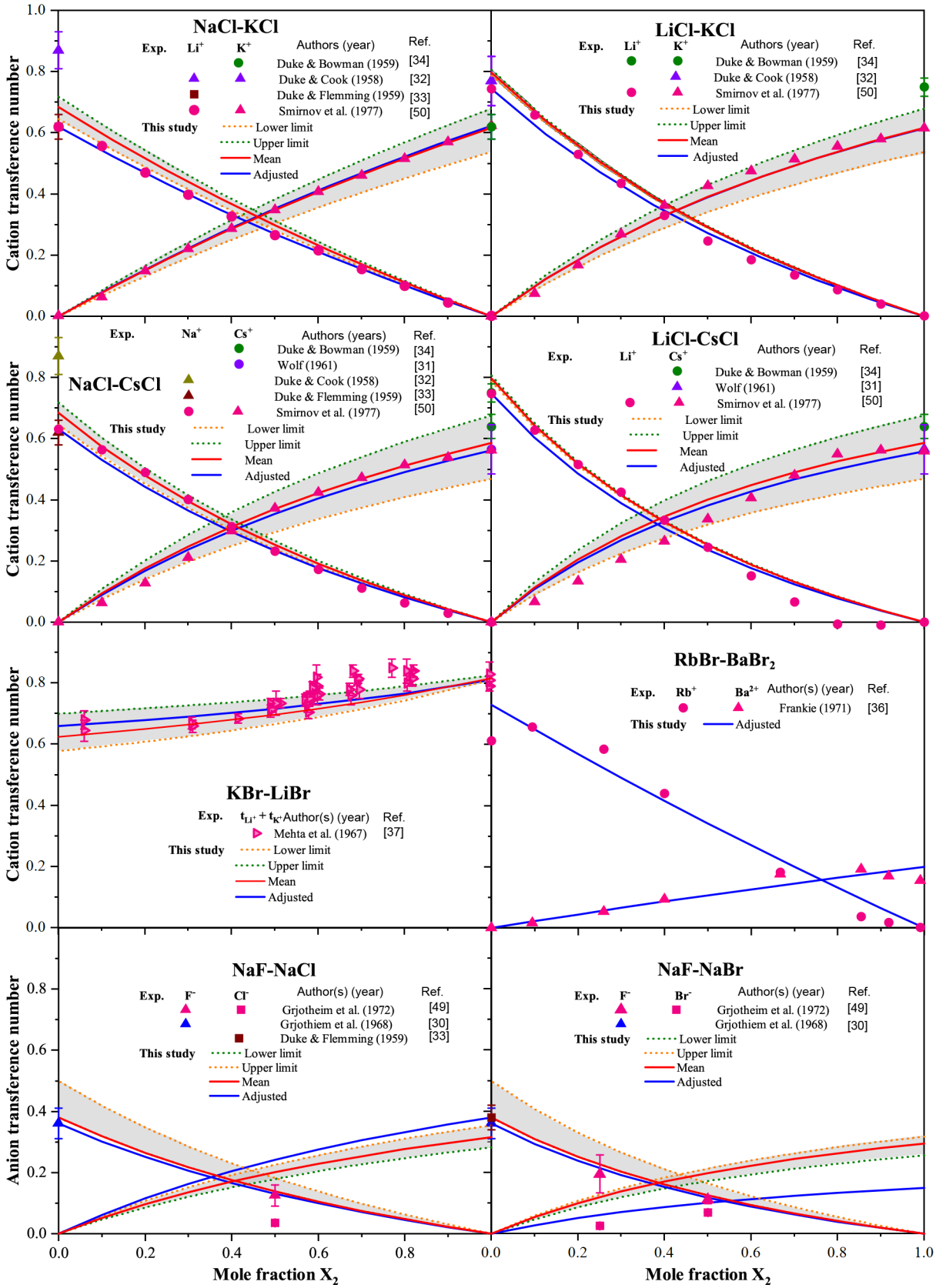

Figure 5. Calculated versus experimental partial cationic transference numbers of the NaCl-KCl, LiCl-KCl, NaCl-CsCl, and CsCl-LiCl systems, and the total cationic transference numbers of the KBr-LiBr and RbBr-$BaBr_2$ systems, along with the comparison of calculated and experimental partial anionic transference numbers of the NaF-NaCl, NaF-NaBr systems. The blue solid line represents the calculated transference numbers based on the experimental transference number for the end members, while the red solid line represents the raw prediction considering the Parrinello-Tosi

https://doi.org/10.1021/acsomega.4c09587
ACS Omega 2025, 10, 10272−10282

Figure 5. continued

temperature-dependent radius.[28] The shadow represents the upper and lower boundaries of the model, corresponding to the maximum deformed and undeformed electronic clouds of the anion, respectively. Experimental data sources: refs 30−34, 37, 49, and 50.

suggested to potentially result in the formation of short-lived complexes in LiCl/CsCl molten mixtures. These complexes, represented as $LiCl_n^{(n-1)^-}$ and $CsCl_n^{(n-1)^-}$ $(1 < n \lesssim 7)$, typically have a lifespan of a few picoseconds. In this scenario, to explain the anomalous behavior of t_{Li^+}, $LiCl_4^{3^-}$ should be predominantly formed above about $X_{CsCl} = 0.6$ and Cs^+ remains free in the second coordination sphere of Cl^-. This scenario is to explain the composition dependence of the transference number of Li^+ within LiCl-CsCl melts and its deviation from the linear dependence with LiCl volume fraction, assuming the experimental data reported by Smirnov et al.[50] are reliable for LiCl-CsCl. If so, why these short-lived complexes impact the transference number and not other transport and dynamics properties still has to be explained and discussed in subsequent work.

Lastly, let us explore molten compounds containing a divalent cation paired with a monovalent anion (e.g., $MgCl_2$, $CaCl_2$, etc.), which have been extensively studied in the literature. By examining these compounds, in addition to those discussed earlier, we encompass a broad spectrum of molten salts with extensive experimental observations. Similar to monovalent cation-based compounds, assumption **As.2** remains relevant in this case, but it is first essential to thoroughly examine the definition of the effective diffusional cross-section of the divalent cation in this context. A molten compound composed of a divalent alkaline earth, a transition, or a post-transition metallic cation, along with a halogen anion, exhibits a complex local structure characterized by the formation of intricate coordination complexes. For instance, in the molten mixture of $MgCl_2$ and $ZnCl_2$, Mg^{2+} and Zn^{2+} ions associate with Cl^- ions to generate substantial complexes of the type $Mg(Zn)Cl_n^{(n-2)^-}$ anions. In this context, the effective diffusional cross sections of the metal cation drastically increase compared to that of the halogen anion. Considering the charge and stoichiometric balance, the complex state of the cation can be treated similarly to two anions simultaneously. In this scenario, the effective cross-section of the cation is represented as

$$\Gamma^{\text{coll.}}_{m^{2+}} = 4\pi(2\bar{r}_{m^{2+}})^2 \Rightarrow \mu_{m^{2+}} \propto \frac{1}{(\bar{r}_{m^{2+}})^2} \tag{13}$$

As depicted in Figure 6, the proposed assumption for the effective diffusional cross-section of divalent metals, as given by eq 13 and combined with the new proposed "golden rule", demonstrates a robust predictive capability of the cationic transference number for all the studied compounds. It is worth noting that the calculation does not account for anion deformation. In contrast to alkaline earth metals and lead cations, the polarizing power of zinc can be substantial, which may elucidate the observed underestimation of the current model. Lastly, it is noteworthy that the cationic transference numbers of noncomplexing chlorides based on transition and post-transition metals, particularly AgCl and TlCl, are predicted with appreciable accuracy using eq 9. For AgCl, $t^{calc.}_{Ag^+} = 0.62$ is comparable to $t^{exp.}_{Ag^+} = 0.65 \pm 0.03$ (as reported by Duby and Kellogg).[57] For TlCl, $t^{calc.}_{Tl^+} = 0.49$ shows a good agreement with $t^{exp.}_{Tl^+} = 0.506 \pm 0.004$ (as reported by Duke and Cook).[32]

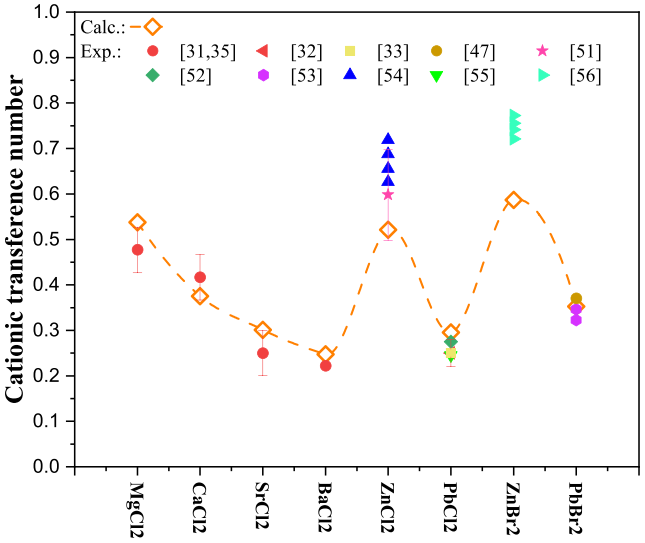

Figure 6. Calculated cationic transference numbers in molten salt compounds, based on divalent metallic cations and monovalent halogens, assume eq 13 for the definition of the effective diffusional cross-section of divalent metals in comparison with experimental work from the literature. Experimental data sources: refs 31−33, 47, and 51−56.

CONCLUSION

In summary, this paper comprehensively examines various aspects of theoretical predictions, encompassing those derived from atomistic simulations along with their inherent limitations. A groundbreaking "golden rule" has been devised, rooted in kinetic theory, and founded upon a straightforward relationship between ion mobility and effective diffusion cross-section. Extensive testing of this novel "golden rule" across a spectrum of molten salt compounds and systems, utilizing available experimental data, has demonstrated its remarkably accurate predictive capacity, consistently aligning with experimental margins of error. This proposed methodology emerges as a promising contender for rapidly and precisely forecasting ion transference numbers in numerous systems where empirical data remain scarce, offering invaluable insights for practical and industrial applications.

In principle, the proposed "golden rule" can be employed to estimate the transference number in complex molten salt systems and even in room-temperature organic molten salts provided that the size of complex anions and polymers can be calculated (or estimated) with appreciable accuracy. The effectiveness of the anionic radius, which accounts for its deformability by considering both the effective electronegativity and the effective polarizability, remains a challenge. This aspect will be assessed in subsequent work for complexing both molten salts and ionic liquids or deep eutectic electrolytes.

ASSOCIATED CONTENT

Supporting Information

The Supporting Information is available free of charge at https://pubs.acs.org/doi/10.1021/acsomega.4c09587.

https://doi.org/10.1021/acsomega.4c09587
ACS Omega 2025, 10, 10272−10282

Comprehensive details on the simulations conducted, including the specific force field descriptions used in the analysis. It elaborates on the model parameters such as ionic radius, electronegativity, and polarizability, essential for accurate computational modeling. Additionally, the document includes calculated values for self-diffusion coefficients and equilibrium density. It also presents a complete set of Onsager phenomenological coefficients (L_{ij}), which are critical for understanding transport properties within the system. All the relevant data and methodologies (PDF)

AUTHOR INFORMATION

Corresponding Author

Aïmen E. Gheribi − *Department of Mechanical, Industrial and Aerospace Engineering, Concordia University, Montreal, Quebec H3G 1M8, Canada;* orcid.org/0000-0002-5443-2277; Email: aimen.gheribi@concordia.ca

Complete contact information is available at: https://pubs.acs.org/10.1021/acsomega.4c09587

Notes

The author declares no competing financial interest.

ACKNOWLEDGMENTS

This research was supported by funds from the Natural Sciences and Engineering Research Council of Canada (NSERC). The atomistic simulations were performed on the supercomputer Narval, managed by Calcul Québec (calculquebec.ca) and the Digital Research Alliance of Canada (alliancecan.ca). We also acknowledge Dr. Anh-Thu Phan for her assistance during the preparation of the manuscript.

REFERENCES

(1) Gaune-Escard, M.; Haarberg, G. *Molten Salts Chemistry and Technology*; Wiley, 2014.

(2) Fellner, P.; Híveš, J.; Thonstad, J. In *Light Metals 2011*; Lindsay, S. J., Ed.; Springer International Publishing: Cham, 2016; pp 513−516.

(3) Janz, G. J. In *Molten Salts Handbook*; Janz, G. J., Ed.; Academic Press, 1967; pp 342−355.

(4) Morand, G.; Hladik, J. *Electrochimie des sels fondus*; Collection de monographies de chimie; Masson et Cie, 1969; v. *1*.

(5) Laity, R. W. *Ion mobility in molten salts*; report no. COO-3514-1; US Atomic Energy Commission; 1971.

(6) Petrucci, S. *Ionic Interactions: From Dilute Solution to Fused Salts*; Physical Chemistry: A Series of Monographs; Elsevier Science, 2012.

(7) Sindzingre, P.; Gillan, M. J. A computer simulation study of transport coefficients in alkali halides. *J. Phys.: Condens. Matter* **1990**, *2*, 7033−7045.

(8) Onsager, L. Reciprocal Relations in Irreversible Processes. I. *Phys. Rev.* **1931**, *37*, 405−426.

(9) Gheribi, A. E.; Machado, K.; Zanghi, D.; Bessada, C.; Salanne, M.; Chartrand, P. On the determination of ion transport numbers in molten salts using molecular dynamics. *Electrochim. Acta* **2018**, *274*, 266−273.

(10) Lemons, D. S.; Gythiel, A. Paul Langevin's 1908 paper "On the Theory of Brownian Motion" ["Sur la théorie du mouvement brownien," C. R. Acad. Sci. (Paris) 146, 530—533 (1908)]. *American Journal of Physics 1997* **1997**, *65*, 1079−1081.

(11) Langevin, P. Sur la théorie du mouvement brownien [On the Theory of Brownian Motion]. *C. R. Acad. Sci. (Paris)* **1908**, 533.

(12) Sundheim, B. R. Transference numbers in molten Salts. *J. Phys. Chem.* **1956**, *60*, 1381.

(13) Merlet, C.; Madden, P. A.; Salanne, M. Internal mobilities and diffusion in an ionic liquid mixture. *Phys. Chem. Chem. Phys.* **2010**, *12*, 14109−14114.

(14) Salanne, M.; Marrocchelli, D.; Watson, G. W. Cooperative Mechanism for the Diffusion of Li+ Ions in LiMgSO4F. *J. Phys. Chem. C* **2012**, *116*, 18618−18625.

(15) Dünweg, B.; Kremer, K. Molecular dynamics simulation of a polymer chain in solution. *J. Chem. Phys.* **1993**, *99*, 6983−6997.

(16) Yeh, I.-C.; Hummer, G. System-Size Dependence of Diffusion Coefficients and Viscosities from Molecular Dynamics Simulations with Periodic Boundary Conditions. *J. Phys. Chem. B* **2004**, *108*, 15873−15879.

(17) Kikugawa, G.; Nakano, T.; Ohara, T. Hydrodynamic consideration of the finite size effect on the self-diffusion coefficient in a periodic rectangular parallelepiped system. *J. Chem. Phys.* **2015**, *143*, 024507.

(18) Busch, J.; Paschek, D. OrthoBoXY: A Simple Way to Compute True Self-Diffusion Coefficients from MD Simulations with Periodic Boundary Conditions without Prior Knowledge of the Viscosity. *J. Phys. Chem. B* **2023**, *127*, 7983−7987. PMID: 37683293.

(19) Gouverneur, M.; Kopp, J.; van Wüllen, L.; Schönhoff, M. Direct determination of ionic transference numbers in ionic liquids by electrophoretic NMR. *Phys. Chem. Chem. Phys.* **2015**, *17*, 30680−30686.

(20) Fong, K. D.; Self, J.; Diederichsen, K. M.; Wood, B. M.; McCloskey, B. D.; Persson, K. A. Ion Transport and the True Transference Number in Nonaqueous Polyelectrolyte Solutions for Lithium Ion Batteries. *ACS Central Science* **2019**, *5*, 1250−1260.

(21) Zhao, J.; Wang, L.; He, X.; Wan, C.; Jiang, C. Determination of Lithium-Ion Transference Numbers in LiPF6−PC Solutions Based on Electrochemical Polarization and NMR Measurements. *J. Electrochem. Soc.* **2008**, *155*, A292.

(22) Gheribi, A. E.; Salanne, M.; Zanghi, D.; Machado, K.; Bessada, C.; Chartrand, P. First-Principles Determination of Transference Numbers in Cryolitic Melts. *Ind. Eng. Chem. Res.* **2020**, *59*, 13305−13314.

(23) Einstein, A. Über die von der molekularkinetischen Theorie der Wärme geforderte Bewegung von in ruhenden Flüssigkeiten suspendierten Teilchen. *Annalen der Physik* **1905**, *322*, 549−560.

(24) Sutherland, W. A dynamical theory of diffusion for non-electrolytes and the molecular mass of albumin. *London, Edinburgh, and Dublin Philosophical Magazine and Journal of Science* **1905**, *9*, 781−785.

(25) Stokes, G. On the Effect of the Internal Friction of Fluids on the Motion of Pendulums. *Trans. Cambridge Philos. Soc.* **1851**, *9*, 8−106.

(26) Mulcahy, M. F. R.; Heymann, E. On the Nature of Molten Salts and their Mixtures. *J. Phys. Chem.* **1943**, *47*, 485−496.

(27) Shannon, R. D. Revised effective ionic radii and systematic studies of interatomic distances in halides and chalcogenides. *Acta Crystallogr., Sect. A* **1976**, *32*, 751−767.

(28) Abramo, M. C.; Caccamo, C.; Pizzimenti, G.; Parrinello, M.; Tosi, M. P. Ionic radii and diffraction patterns of molten alkali halides. *J. Chem. Phys.* **1978**, *68*, 2889−2895.

(29) Yang, H.; Gallagher, R.; Chartrand, P.; Gheribi, A. E. Development of a molten salt thermal conductivity model and database for advanced energy systems. *Sol. Energy* **2023**, *256*, 158−178.

(30) Grjotheim, K.; Matiasovsky, K.; Myhre-Andersen, S.; Oye, H. A. Transport numbers in molten fluorides—I. Sodium fluoride. *Electrochim. Acta* **1968**, *13*, 91−98.

(31) Wolf, E. D. Transport numbers in fused cesium chloride. *J. Electrochem. Soc.* **1961**, *108*, 811.

(32) Duke, F. R.; Cook, J. P. A nonvisual method for transport numbers in pure fused salts. II. *Iowa State Coll. J. Sci.* **1958**, *33*, 81.

(33) Duke, F. R.; Fleming, R. A. Transport numbers and ionic mobilities in the system potassium chloride-lead chloride. *J. Electrochem. Soc.* **1959**, *106*, 130.

(34) Duke, F. R.; Bowman, A. L. Transport numbers in pure fused salts. *J. Electrochem. Soc.* **1959**, *106*, 626.

(35) Wolf, E. D.; Duke, F. R. Transference numbers and ion association in pure fused alkaline earth chlorides. *J. Electrochem. Soc.* **1963**, *110*, 311.

(36) Franke, G. R. Electrical transport properties of the molten rubidium bromide-barium bromide system. Ph.D. thesis, Purdue University, 1971.
(37) Mehta, O. P.; Lantelme, F.; Chemla, M. Transport ionique dans les bromures alcalins fondus. *Rev. Int. Hautes Tempér. et Réfract.* **1967**, *4*, 21−27.
(38) Ahmed, S. N. In *Physics and Engineering of Radiation Detection*, 2nd ed.; Ahmed, S. N., Ed.; Elsevier, 2015; pp 65−155.
(39) Salanne, M.; Madden, P. A. Polarization effects in ionic solids and melts. *Mol. Phys.* **2011**, *109*, 2299−2315.
(40) Leidens, L. M.; Maia da Costa, M. E. H.; Figueroa, N. S.; Barbieri, R. A.; Alvarez, F.; Michels, A. F.; Figueroa, C. A. On the physicochemical origin of nanoscale friction: the polarizability and electronegativity relationship tailoring nanotribology. *Phys. Chem. Chem. Phys.* **2021**, *23*, 2873−2884.
(41) Fajans, K. Struktur und Deformation der Elektronenhüllen in ihrer Bedeutung für die chemischen und optischen Eigenschaften anorganischer Verbindungen. *Naturwissenschaften* **1923**, *11*, 165−172.
(42) Labrie, R. J.; Lamb, V. A. Transference Numbers in Pure Molten Sodium Nitrate. *J. Electrochem. Soc.* **1963**, *110*, 810.
(43) Duke, F. R.; Laity, R. W. Transport numbers in pure fused salts: lead chloride, lead bromide, thallous chloride, and silver nitrate. *J. Electrochem. Soc.* **1958**, *105*, 97.
(44) Duke, F. R.; Victor, G. Transport Numbers of Some Pure Fused Nitrates and Nitrites. *J. Electrochem. Soc.* **1963**, *110*, 91.
(45) Honig, E. P. Transport Phenomena in Fused Salts, Electromigration, Self Diffusion and Electrodiffusion in Ionic Melts. PhD thesis, 1964; Amsterdam.
(46) Bloom, H.; James, D. W. Anion Transport Number in Pure Molten Silver Nitrate. *J. Phys. Chem.* **1959**, *63*, 757.
(47) Duby, P.; Kellogg, H. Measurement of "Pressure-EMF" in Pure Fused Salts. *J. Electrochem. Soc.* **1963**, *110*, 349.
(48) Jenkins, H. D. B.; Thakur, K. P. Reappraisal of thermochemical radii for complex ions. *J. Chem. Educ.* **1979**, *56*, 576.
(49) Grjothem, K.; Haugerød, O.; Stamnes, H.; Oye, H. Transport numbers in molten fluorides—II. Mixtures between NaF-NaCl and NaF-NaBr. *Electrochim. Acta* **1972**, *17*, 1547−1556.
(50) Smirnov, M. V.; Aleksandrov, K. A.; Khokhlov, V. A. Diffusion potentials and transport numbers in molten alkali chlorides and their binary mixtures. *Electrochim. Acta* **1977**, *22*, 543−550.
(51) Lundén, A. Transport Numbers in Pure Fused Zinc Chloride. *J. Electrochem. Soc.* **1962**, *109*, 260.
(52) Murgulescu, I. G.; Marta, L. Investigation of Ionic Transport Numbers in Molten Lead Chloride ($PbCl_2$). *Acad. Rep. Populare Romine Studii Cercetari Chim.* **1960**, *8*, 375.
(53) Laity, R. W.; Duke, F. R. Transport Numbers in Pure Fused Salts: Lead Chloride, Lead Bromide, Thallous Chloride, and Silver Nitrate. *J. Electrochem. Soc.* **1958**, *105*, 97.
(54) Fischer, W.; Klemm, A. Die aussere Uberfuhrung von geschmolzenem TlCl und ZnCl2. *Zeitschrift fur Naturforschung A* **1961**, *16*, 563−568.
(55) Duke, F. R.; Laity, R. W. The measurement of transport numbers in pure fused salts. *J. Phys. Chem.* **1955**, *59*, 549.
(56) Sjöblom, C.-A.; Andersson, J. External Transport Numbers in Molten Zinc Bromide. *Zeitschrift für Naturforschung A* **1968**, *23*, 235.
(57) Duby, P.; Kellogg, H. H. Transport Numbers in Pure Molten AgNO3 and AgCl by a Simplified Weighing Method. *J. Electrochem. Soc.* **1964**, *111*, 1181.

https://doi.org/10.1021/acsomega.4c09587
ACS Omega 2025, 10, 10272−10282